Revisiting the 1897 Shillong and 1905 Kangra earthquakes in northern India: Site Response, Moho reflections and a Triggered Earthquake

Susan E. Hough(1), Roger Bilham(2), Nicolas Ambraseys(3), and Nicole Feldl(2)

(1)U.S Geological Survey, Pasadena, California USA
(2)University of Colorado, Boulder, Colorado USA
(3)Imperial College, London, UK

Abstract

Re-valuated instrumental magnitudes and intensity distributions for the Mw8.0 Shillong Plateau earthquake of 1897 and the Mw7.8 Kangra earthquake of 1905, combined with newly available geodetic constraints on rupture geometries, allow us to compare observed distributions of intensity with those predicted from theoretical models for shaking produced by each earthquake. The difference between predicted and observed shaking is interpreted in terms of the site response of the Ganges and Brahmaputra basins. As expected, these comparisons identify regions of enhanced shaking near the main rivers. We infer amplifications of 1-2 intensity units, corresponding to an amplification factor of 2-4 in peak ground acceleration. We also find two unexpected results in our comparison of observed and predicted shaking from the Kangra earthquake: 1) The epicentral region is surrounded by a halo of enhanced intensity at 150-200 km radius and 2) The Dehra Dun region was the locus of a broad region of anomalously high intensities. We interpret the former result as the signal from post-critical Moho reflections and the latter observation as a probable second large earthquake (M>7) at 30-50 km depth triggered within minutes of the 1905 mainshock. These results have important consequences from future earthquakes in the Himalaya.

Introduction

Several recent studies have provided new estimates of magnitude, rupture parameters, and shaking intensity for the 1897 Assam and the 1905 Kangra earthquakes in northern India. The dense spatial coverage of these data provides substantial information about the distribution of shaking in the alluvial plains of northern India that can be used to evaluate past and future great Himalayan earthquakes as well as to address unresolved general issues related to both events.

The magnitudes of the 1897 and 1905 earthquakes listed in early catalogues vary by 0.5 magnitude units. The re-evaluated instrumental data indicate the 1897 earthquake was Ms=8.0±0.1 (Ambraseys, 1999), and the 1905 earthquake was Ms=7.8±0.05 (Ambraseys and Bilham, 2000).

The observed shaking intensity distribution for the 1897 earthquake was originally evaluated by Oldham (1899), and for the 1905 earthquake by Middlemiss (1905, 1910). These observations have now been supplemented by numerous additional accounts found in newspapers, government reports and materials unavailable to these authors, and these have been re-evaluated using the MSK scale of intensities. In all 282 unequivocal MSK intensities were assigned for the 1897 earthquake (Figure 1a, Ambraseys and Bilham, 2003), and 523 for the 1905 earthquake (Figure 1b, Ambraseys and Douglas, 2003). The new evaluations take into account building styles and ignore accounts for which reliable intensities cannot be assessed. In particular, locations where damage was associated with liquefaction were not included in assessments of intensity. It is now recognized that liquefaction tends to occur over a large range of moderate to high intensities in regions where saturated sediments are present, resulting in building damage caused by foundation failure, rather than by the accelerations that caused the liquefaction. It is typically impossible to assign a precise intensity to these observations.

The re-evaluated intensity data, and the revised instrumental magnitudes for these two earthquakes, provide a key to interpreting intensity data from numerous earlier historical earthquakes for which only intensity data are available.

Rupture geometry for the 1897 and 1905 earthquakes

Geodetic data combined with geological observations of secondary faulting in the epicenter of the 1897 Shillong Plateau earthquake provide strong constraints on rupture geometry, indicating 16±5 m of reverse slip on a 110±10-km ESE fault, corresponding to Mw=8.1±0.1 (Bilham and England, 2001). The down-dip width of the causal rupture is the least well-constrained parameter in the solution but it appears to have slipped on a 50±5° SSW dipping fault from 35 km to 9 km depth, extending through much of the crust. This subsurface slip stressed the shallower regions of the Shillong plateau resulting in 10 m of normal faulting on the Chedrang fault observed by Oldham (1899).

In contrast, geodetic data for the Kangra earthquake sample only the SW edge of the inferred 1905 rupture and provide weak constraints for an inferred shallow-dipping thrust fault with less than 5 m of slip (Wallace et al., 2003). Several authors have used leveling data from the Dehra Dun region to support the notion that rupture extended 250 km SE of the epicenter, consistent with a region of high intensity shaking recorded in the region of Dehra Dun (e.g. most recently Yeats, 1992). A re-evaluation of the raw leveling data shows, however, that the data used in these studies are significantly contaminated by systematic errors (Bilham, 2001) and that there was probably little or no uplift in the Dehra Dun region. The absence of significant uplift or horizontal deformation (Turner, 1907) at Dehra Dun constrains the rupture length to be less than 180 km. This is consistent with the revised magnitude of Mw=7.8, which suggests the rupture length was no more than 110 km, given a probable 50-70 km rupture width (Wallace et al. 2002). The rupture presumably terminated to the southwest near the mapped location of the Jawalmucki thrust fault (Powers et al., 1998). The inferred rupture parameters for 1897

and 1905 are used below as input in computer simulations that generate synthetic shaking intensity maps for each earthquake.

Previous attempts to assess the location, extent and strike of the 1905 rupture area based on intensity data published by Middlemiss (1910) show a zone of intense destruction near the town of Kangra (RF VIII-X), and an isolated zone of lower intensity (RF VIII) centered 250 km to the SW near the town of Dehra Dun. For many years the inflated magnitude assigned by Richter to this earthquake (Ms=8.0) supported the widely held belief that the rupture zone corresponded approximately to the area of RF intensity VII shaking that enveloped these two high intensity regions.

The reality of the intervening region of lower intensity shaking between these two regions of damage has been investigated in several studies (Seeber and Armbruster, 1972; Molnar, 1987). These studies conclude that although Middlemiss's coverage of the intervening region was limited to two traverses, it would have revealed high intensity shaking had any been present. The revised and expanded MSK data confirm that the low intensity region is not an artifact caused by poor spatial sampling (Figure 1b).

For the purposes of comparing Middlemiss' contours with the re-evaluated MSK intensities we contoured their distribution using a purely mathematical algorithm. Contouring is done using the GMT routine "surface" (see Wessel and Smith, 1991); this routine produces contours of randomly spaced spatial data, z(x,y), by solving

$$(1-T)*L(L(z)) + T*L(z) =0$$

where T is a tension factor and L is the Laplacian operator. We use T=1, which provides a harmonic solution with no maxima or minima away from control points. Our contours resemble the older Rossi-Forel isoseismals, although our larger number of intensity reports provides additional detail. The similarities between Middlemiss' contours and the contours in Figure 1b confirm the essential features of the 1905 earthquake: a low intensity region separates the epicentral rupture zone from a zone of high intensity 250 km to the SW.

We found a tendency for Middlemiss' higher isoseismals to include unjustifiably large areas, a conclusion derived also for Oldham's isoseismals contoured for the 1897 earthquake (Ambraseys and Bilham, 2003). This bias is caused by extensive building damage at relatively modest levels of shaking with no graded intensification of damage towards higher levels of shaking. A comparison of Middlemiss' areas of Rossi-Forel shaking with those of inferred MSK shaking shows them to be approximately one intensity unit too high above Intensity VIII and a half intensity too high above intensity VII. For lower intensities we find the areas comparable.

Predicted Intensity Distributions

As was demonstrated by Hough et al. (2002) for the 2001 Bhuj earthquake, one can use ground motion modeling methods to predict the distribution of ground motions from a given fault model and, using established relationships between ground motions and intensities (Wald et al., 1999), convert this into a predicted damage map. Following the Hough et al. (2002) approach, we calculate predicted hard-rock damage patterns from both the 1897 and the 1905 earthquakes using rupture models constrained from geodetic data and other available information. We use the method of Beresnev and Atkinson (1997), a well-calibrated, semi-stochastic approach that includes finite-fault effects to the extent that the source is distributed (finite-fault phase effects are not modeled with this approach). We also use the attenuation results of Singh et al. (1999) for regional Q(f).

One key unknown in the Beresnev and Atkinson (1997) approach is the "strength factor," which is related to slip velocity. For both earthquakes we initially choose the same value that Hough et al. (2002) obtained for the Bhuj earthquake: 1.6. Although this value cannot be determined precisely without quantified ground motion estimates, it can be adjusted based on the overall intensity pattern. For the 1897 earthquake, we find that the value of 1.6 provides a very good fit to the extent of the region over which light damage occurred. For the 1905 earthquake, a better fit is obtained with a lower value: 1.2. For the 1905 earthquake, a better fit is obtained with a lower value: 1.2. To include the effect of the Chedrang fault rupture in our predicted shaking map for the Kangra earthquake, we model a second event with the appropriate rupture parameters. The combined intensity map is then determined by choosing, at each point, the higher of the values predicted from the Chedrang and Oldham fault ruptures. This approach presumably provides a lower bound for the combined shaking level, as two distinct ruptures are expected to prolong the duration of strong ground motion at many sites, and thus to potentially generate more severe damage than two distinct earthquakes.

Figures 2a and 2b show the observed and predicted intensity distributions for the 1897 and 1905 earthquake. Figures 3a and 3b show the residuals: calculated simply as the observed minus predicted intensity values.

For the Shillong earthquake, we obtain a broad region of amplified intensities corresponding to the Ganges Basin (Figure 3a), consistent with the expectation of amplification at soft-sediment sites. We do not observe amplification along the Brahmputra River, but this is because Ambraseys and Bilham (2003) do not assign intensity values for the many sites along this river for which there was documented liquefaction, but insufficient information to assign intensity. On Figure 3a we indicate the sites at which liquefaction was observed. Many of these are along the Bhramaputra River; it thus appears that shaking was amplified in these locations as well, although the observations are not sufficient to quantify it. Throughout the Ganges Basin, however, we find consistent amplification of 1-2 intensity units. As discussed by Hough et al. (2002) this implies a peak ground acceleration amplification of 2-4.

The intensity residuals from the 1905 earthquake reveal a more complex pattern than those from the 1897 event (Figure 3b). Our preferred choice of strength factor results in

a good overall match to the shaking distribution. However, several features of the residual map are found to be insensitive to changes in modeling parameters such as the strength factor and detailed rupture geometry.

From Figure 3b we make the following observations: 1) Shaking in the main rupture zone is overpredicted, 2) amplified shaking is observed near the banks of rivers in the Ganges, and in the Kashmir Valley, 3) a faint region of increased intensity is evident surround the epicenter at a distance of roughly 180 km, and 4) a broad region of high residuals is found near Dehra Dun; this is displaced 20 km to the east from a high intensity zone contoured by Middlemiss. These observations are discussed in turn below.

In contrast to the results for the 1897 event, our modeling predicts stronger near-field shaking than that observed. It is possible that this reflects a bias in the intensity assignments: if the only structures damaged in an earthquake are of construction types that are highly vulnerable to damage, it is impossible to ascertain if very high shaking occurred. However, the 1905 mainshock is inferred to have been a low-angle thrust rupture of the main Himalayan decollement fault, and several recent studies suggest that other shallow thrust events, most notably the 1999 Chi-Chi, Taiwan earthquake, generated relatively low near-field peak accelerations (e.g., Boore, 2001). Our results are consistent with this hypothesis.

Our second observation, of amplified shaking along rivers and in valleys, is again consistent with expectations for significant amplifications at soft-sediment sites. The degree of amplification is consistent with that inferred for the 1897 earthquake.

SmS reflected wave from the Moho?

The faint high-intensity "halo" surrounding the mainshock extends both to the west of the mainshock, on sediment sites, and to the east, on hard-rock sites. We interpret this pattern as evidence that post-critical Moho reflections are large enough to contribute in a significant way to damage patterns. The geometry that leads to these reflections is illustrated in Figure 4. Previous studies have argued for such an effect in other earthquakes beginning with the 1989 Loma Prieta, California earthquake (Somerville and Yoshimura, 1990). Somerville and Yoshimura showed that SmS arrivals were larger than the direct S arrivals at distances of 50-100 km; later studies (e.g., Mori and Helmberger, 1996) have found similar results. Although a detailed crustal model would be required for precise ray-tracing, tomographic studies indicate that the Moho is located at approximately 40 km along the Himalayan front (Sheehan et al, 2003); high amplitude SmS waves at distances of 100-200 km are thus consistent with this interpretation.

While a number of studies have found evidence that post-critical Moho reflections contribute to damage patterns, past studies have relied on far fewer data points than are provided by our dense sampling. For perhaps the first time, dense macroseismic data from the Kangra earthquake have illuminated the full spatial distribution of SmS arrivals. These results suggest a deeper Moho to the northeast of the mainshock than to the

southwest, a hypothesis that will be testable when crustal structure is known in more detail.

A faint halo is suggested in the intensity residuals calculated for the 1897 earthquake, especially to the south and west of the epicenter. The signal is less prominent, however, than that of the 1905 earthquake, presumably due to the latter event's substantially deeper epicenter and different mechanism. The Kangra earthquake presumably occurred on a shallow dipping thrust at 6-12 km depth largely on, and parallel to, the upper surface of the Indian plate, whereas the Shillong earthquake ruptured through the plate from at least 35 km depth on a steep reverse fault that terminated far below the surface.

Perhaps the most conspicuous feature in the residual 1905 intensity plot is the roughly circular region of high intensities near Dehra Dun, centered slightly to the west of Middelmiss' intensity VIII outlier. The circular nature of the aftershock pattern is suggestive of a triggered earthquake rather than sedimentary basin amplification since at least half of the high intensity observations are found north of the Ganga Plain within the Himalayan foothills. The (inferred) triggered earthquake location is close to the SmS "halo" discussed earlier, suggesting that these arrivals might have contributed to the triggering of the subsequent event.

A second earthquake in the Dehra Dun region has been suggested by previous authors who have explored possible causes for the region of isolated high intensities in the Rossi-Forel contours (e.g., Chander, 1988). Had a separate shock occurred it would have to have been close to the time of the mainshock for people to not have reported two separate shocks. The epicenter of this triggered earthquake is apparently 29.0°N, 78.7°E with an uncertainty of ±0.5°.

Although the intensity residual generated by the (inferred) triggered earthquake is dramatic, the intensity distribution reveals a broad region of relatively modest shaking in the Dehra Dun region. Using our modeling approach to match this pattern, we conclude that the earthquake must be large (Mw upwards of 7.0) and deep (depth upwards of 30 km). There is, however, a trade-off in the modeling between magnitude and depth; we cannot distinguish between, say, a Mw7 event at 30 km depth and a Mw7.5 event at 50 km depth.

If a remotely triggered earthquake of Mw~7 did occur at 30 km depth, the relatively recent 1988 Bihar-Nepal earthquake might represent an analog for this event. The PDE magnitude of this earthquake is Mw6.7 and it occurred on a NE-trending strike-slip fault near the base of the India plate (Dikshit and Koirala, 1983; GSI, 1993; Chen and Kao, 1996).

No horizontal deformation was detected near Dehra Dun in 1905 (Burrard, 1906; Turner, 1907) and although 15 cm of apparent uplift has been described in numerous articles that interpret this as coseismic defomation, the raw leveling data are contaminated by systematic errors (Bilham, 2000), and it is doubtful that any vertical deformation

occurred. Hence the geodetic data, once considered an important constraint on mainshock rupture, are unable to substantiate the possible occurrence of a triggered earthquake near Dehra Dun. The leveling data are especially unhelpful to resolve the parameters of a deep earthquake, for which the surface deformation will be muted, and will be expressed by a long surface wavelength.

To address further the question of a possible triggered earthquake we have searched for early instrumental recordings of the 1905 earthquake. Although instrumental recordings from this date are sparse, we were able to locate several records from which arrivals can be identified with some confidence. Two P-wave arrivals are evident at Colaba Observatory (Bombay) in the first minute of the earthquake, and two distinct S-wave arrivals separated by about 6-7 minutes are suggested in the Wiechert recording from Gottingham. The best evidence, however, comes from the station at Leipzig: a damped Wiechert instrument (Figure 5). This record reveals clear evidence of a second, high-frequency S-wave group, about 7 minutes after the first S arrivals. The record moreover suggests that the sS-S time of the second event is larger than the sS-S time of the first event, consistent with our inference that the triggered earthquake was considerably deeper than the first.

An additional source of epicentral shaking data is found in the horizontal-force magnetogram recorded at Dehra Dun recorded on a chart advancing at approximately 15 mm/hour (Thomas, 1907). The record saturates for 8 minutes following the arrival of surface waves from the mainshock, but distinct shocks occur at 11.3 m, 19.7 m, 25.6 m and 43.5 m after this first arrival. The times in the following abstract from Thomas (1907) are cited in Madras local time (GMT-5:21) indicating the arrival of Raleigh waves at Dehra Dun at 00:51±1m GMT. Middlemiss infers an origin time of 06:09 or 00:48.

"At Dehra the effect begins sharply with a maximum (the oscillation being so rapid as to fail to register photographically) at 6h 11.6m; the maximum continues till 6h 19.8m, a period of 8.2 minutes; this is followed by a period of slower oscillation for 3.1 minutes, when a second sharp shock was recorded at 6h 22.9 m : the magnet continued oscillating until 6h 37.3m, a period of 25.7 minutes, during which there were in addition to the principal shock 3 others recorded, namely, at 6h 22.9, 6h 31.3, and 6h 36.2m. A further disturbance occurs at 6h 55.1 m (duration about 1.4 minutes) which is the only aftershock noted at Barackpore" (near Calcutta).

Because of the initial saturation of the instrument the data do not provide any information about separate shocks that might have occurred within 8 minutes of the mainshock. However, the noted times of the later events can be used to constrain the times of early large aftershocks, which we use in the following section as a guide to the interpretation of anecdotal accounts.

Felt and recorded aftershocks in 1905

Numerous felt reports of aftershocks are listed by Middlemiss (1910) who considers their reported times to be unreliable. However, if we assume that observers noted only the strongest aftershocks, it is possible to synchronize these reports using the aftershocks

recorded by the magnetogram. In Figure 6 we show the locations of reported aftershocks reported during the 15 minutes following the mainshock; these are plotted spatially and labeled according to the minute they were felt. The mean location of reports (independent of intensity) for two consecutive 8 minute windows are calculated to lie 20-100 km SE of Dehra Dun, near the inferred location of the secondary shock (Table 1).

Because the Kangra epicentral region was severely damaged, few people were able to document the timing of aftershocks. The locations listed in Table 1 may thus be biased away from the mainshock epicenter. Together with the scant distribution of quantitative observations and their concentration in a few urban centers, this leads to a probable bias toward Dehra Dun. Notwithstanding these limitations, the results suggest that the Dehra Dun region experienced either an anomalously large number of felt aftershocks shortly after the mainshock, or a large number of poorly timed observations of a single large aftershock, within fifteen minutes of the mainshock arrival.

Conclusions

Macroseismic observations from two key historic earthquakes in the Himalayan region reveal unexpected details of the nature of the ground motions generated by these events. Using available geodetic and other information to constrain rupture models, we are able to predict the distributions of shaking from the events and to compare these results to the observed intensities. We obtain several interesting results, including maps of sediment-induced amplification in the Ganges Basin and elsewhere, as well as compelling evidence that the 1905 Kangra mainshock was followed by a subsequent, remotely triggered earthquake in the Dehra Dun region. The depth of this triggered earthquake (30-50 km) requires it to have occurred below the plate boundary, and probably at the base of the Indian plate.

Our results underscore seceral important conclusions about triggered earthquakes. First, while small remotely triggered earthquakes occur commonly in geothermal and volcanic regions (e.g., Hill et al., 1993), large triggered earthquakes are possible. As this study demonstrates, large, early triggered events can be very difficult to identify without modern instrumental data. We note, however, that there is evidence for triggered earthquakes following both the 1934 Mw8.0 Bihar-Nepal earthquake and the 2001 Mw7.6 Bhuj earthquake. The former event was followed the next day by a M5.6 earthquake approximately 170 km to the north of the mainshock; the Bhuj earthquake was followed three days later by a M4.3 earthquake 12.4N 77.3W, over 1400 km south of the epicenter. The distance between the 1934 mainshock and inferred triggered event is comparable to that between the Kangra mainshock and Dehra Dun event, again suggesting that triggered earthquakes may occur preferentially at distances where SmS waves generate high-amplitude arrivals.

The triggered earthquake identified in this study, like the 1988 Udaypur, Nepal, earthquake, underscores the important conclusion that an important source of seismic hazards in the Himalaya lies not only on slip on the plate boundary, but from earthquakes that respond at depth to the bending or unbending of the descending plate (e.g., Bilham et al., 2003).

Acknowledgements

Support for two of the authors (RB and NF) was provided by NSF EAR0003449 and EAR0229690.

Bibliography

Ambraseys, N. and R. Bilham, A note on the Kangra Ms=7.8 earthquake of 4 April 1905, Current Science, 79, 101-106, 2000.

Ambraseys, N. and R. Bilham, Re-evaluated intensities for the great Assam earthquake of 12 June 1897, Shillong, India, Bull. Seism. Soc. Am., 93, 2003.

Ambraseys, N. N. and J. Douglas, 2003. Magnitude calibration of north Indian earthquakes, *Geophys. J. Int* in the press.

Beresnev, I.A. and G.M. Atkinson, Generic finite-fault model for ground-motion prediction in eastern North America, Bull. Seism. Soc. Am., 89, 608-625, 1997.

Bilham, R., Slow tilt reversal of the Lesser Himalaya between 1862 and 1992 at 78°E, and bounds to the southeast rupture of the 1905 Kangra earthquake, Geophys. J. Int (2001) **144**, 1-23.

Bilham, R. and P. England, Plateau pop-up during the great 1897 Assam earthquake, Nature 410, 806-809, 2001.

Bilham, R., K. Wallace, F. Blume, and N. Feldl, Flexure and fragmentation of the Indian plate: mid-plate earthquakes, in, Indo-US Workshop on Seismicity and Geodynamics, National Geophysical Research Institute, Hyderabad, India, 27, 2003.

Boore, D.M., Comparisons of ground motions from the 1999 Chi-Chi earthquake with empirical predictions largely based on data from California, Bull. Seism. Soc. Am., 91, 1212-1217.

Burrard, S. G. (1906). Geodesy, 42-52, *in* Annual Report of the Board of Scientific Advice for India for the Year 1904-05, Government Central Press, Calcutta, 1906. pp. 138.

Chander, R. (1988). Interpretation of observed ground level changes due to the Kangra earthquake, northwest Himalaya, Tectonophysics, 149, 289-298.

Chen, W.-P. and H. Kao, (1996). Seismotectonics of Asia: some recent progress, in the Tectonic Evolution of Asia, ed. A. Yin and T.M. Harrison, Cambridge University Press, 37-54.

Dikshit, A.M. and A. Koirala, (1989). Report on the intensity mapping of Udaypur earthquake of 20 August 1988. HMG Ministry of Industry, Nepal, Dept. of Mines and Geol., Lainchaur, Kathmandu.

Geologic Survey of India, Bihar-Nepal earthquake, August 20, 1988, GSI Special Publication 31, Eds. D.R. Nandy, A.K. Cloudhury, C. Chakraborty, and P.L. Narula, 1993.

Hough, S.E., S. Martin, R. Bilham, and G. Atkinson, The 26 January, 2001 Bhuj, India earthquake: observed and predicted ground motions, Bull. Seism. Soc. Am. 92, 2061-2079, 2002.

Middlemiss, C.S., Preliminary account of the Kangra earthquake of 4th April 1905, Mem. Geol. Soc. India, 32, Pt. 4, 258-294, Geol. Surv. India, Calcutta.

Middlemiss, C.S., The Kangra earthquake of 4 April 2005, Mem. Geol. Surv. India 38, 405, 1910.

Molnar, P., The distribution of intensity associated with the 1905 Kangra earthquake and bounds on the extent of rupture, J. Geol. Soc. India, **29**, 221, 1987.

Mori, J. and D. Helmberger, Large-amplitude Moho reflections (SmS) from Landers aftershocks, southern California, Bull. Seism. Soc. Am. 86, 1845-1852, 1996.

Powers, P. M., Lillie, R. J., and Yeats, R. S., 1998, Structure and shortening of the Kangra and Dehra Dun reentrants, Sub-Himalaya, India: *Geol. Soc. Am. Bull.,* **110,** 1010-1027.

Seeber, L. and J.G. Armbruster, Great detachment earthquakes along the Himalayan Arc and long-term forecasting, in Earthquake Predictionan International Review, eds. D.W. Simpson and P.G. Richards, Maurice Ewing Series, Am. Geophys. U., 4, 259-277, 1981.

Singh, S.K., M. Ordaz, R.S. Dattatrayam, and H.K. Gupta, A spectral analysis of the 21 May 1997, Jabalpur, India earthquake (Mw5.8) and estimation of ground motion from future earthquakes in the Indian shield region, Bull Seism. Soc. Am., 89, 1620-1630, 1999.

Thomas, R. H. (1907) The Magnetic Survey of India 1904-05 p.1-74. *in* Longe, F. B. Extracts from Narrative Reports of Officers of the Survey of India for the season 1904-

05. Survey of India, Government Printing Office, Calcutta.

Turner, H. H., (1907) Triangulation in Baluchistan, No.24 Survey Party (Triangulation) for season 1904-05, **IV**, p.115 *in* Longe, F. B. Extracts from Narrative Reports of Officers of the Survey of India for the season 1904-1905. Government Printing Office, Calcutta, 1907.

Wald, D.J., V. Quitoriano, T.H. Heaton, and H. Kanamori, Relationships between peak ground acceleration, peak ground velocity, and modified Mercalli intensity in California, Earthquake Spectra, 15, 557-564, 1999.

Wallace, K., Rebecca Bendick, Roger Bilham, Frederick Blume, Vineet Gahalaut & Vinod Gaur (2002). Geodetic constraint of the Kangra 1905 Ms=7.8 rupture. EOS, Trans. Am. Geophys. U., abs.

Wesnousky, S. G., Kumar, S., Mohindra, R., and Thakur, V. C. (1999). Holocene slip rate of the Himalayan Frontal Thrust of India, Observations near Dehra Dun: Tectonics, **18**, 967-976.

Wessel, P. and W.H.F Smith, Free software helps map and display data, EOS, Trans. Am. Geophys. U., 72, 441, 445, 1991.

Yeats, R.S., T. Nakata, A. Faraj, M. Fort, M.A. Mirza, M.R. Pandey, and R.S. Stein, The Himalayan frontal fault system, Ann. Tect. 6, 85-98, 1992

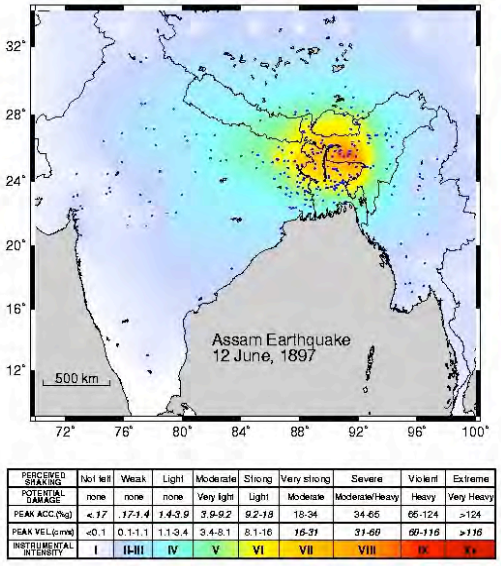

PERCEIVED SHAKING	Not felt	Weak	Light	Moderate	Strong	Very strong	Severe	Violent	Extreme
POTENTIAL DAMAGE	none	none	none	Very light	Light	Moderate	Moderate/Heavy	Heavy	Very Heavy
PEAK ACC.(%g)	*<.17*	*.17-1.4*	*1.4-3.9*	*3.9-9.2*	*9.2-18*	18-34	34-65	65-124	>124
PEAK VEL.(cm/s)	<0.1	0.1-1.1	1.1-3.4	3.4-8.1	8.1-16	*16-31*	*31-60*	*60-116*	*>116*
INSTRUMENTAL INTENSITY	I	II-III	IV	V	VI	VII	VIII	IX	X+

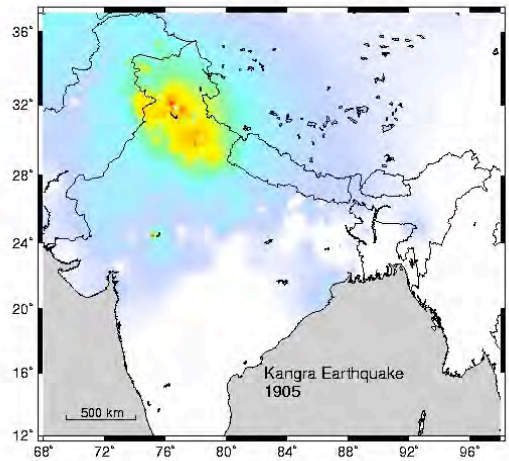

PERCEIVED SHAKING	Not felt	Weak	Light	Moderate	Strong	Very strong	Severe	Violent	Extreme
POTENTIAL DAMAGE	none	none	none	Very light	Light	Moderate	Moderate/Heavy	Heavy	Very Heavy
PEAK ACC.(%g)	*<.17*	*.17-1.4*	*1.4-3.9*	*3.9-9.2*	*9.2-18*	18-34	34-65	65-124	>124
PEAK VEL.(cm/s)	<0.1	0.1-1.1	1.1-3.4	3.4-8.1	8.1-16	*16-31*	*31-60*	*60-116*	*>116*
INSTRUMENTAL INTENSITY	I	II-III	IV	V	VI	VII	VIII	IX	X+

Figure 1. Observed intensity distribution for the 1897 Assam earthquake (1a, left) and 1905 Kangra earthquake (1b, right) as determined by Ambraseys and Bilham (2003) and Ambraseys and Douglass (2004), respectively. Scale bar indicates ground motion values, pga and pgv, that are found to correspond to each intensity level using instrumentally recorded earthquakes in California (Wald et al. 1999).

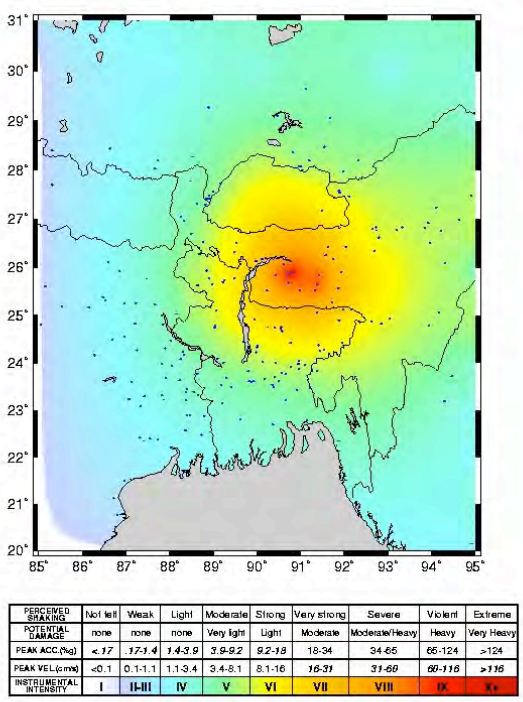

PERCEIVED SHAKING	Not felt	Weak	Light	Moderate	Strong	Very strong	Severe	Violent	Extreme
POTENTIAL DAMAGE	none	none	none	Very light	Light	Moderate	Moderate/Heavy	Heavy	Very Heavy
PEAK ACC.(%g)	*<.17*	*.17-1.4*	*1.4-3.9*	*3.9-9.2*	*9.2-18*	18-34	34-65	65-124	>124
PEAK VEL.(cm/s)	<0.1	0.1-1.1	1.1-3.4	3.4-8.1	8.1-16	*16-31*	*31-60*	*60-116*	*>116*
INSTRUMENTAL INTENSITY	I	II-III	IV	V	VI	VII	VIII	IX	X+

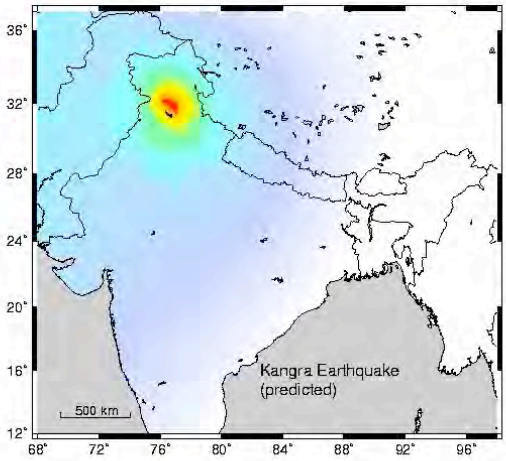

PERCEIVED SHAKING	Not felt	Weak	Light	Moderate	Strong	Very strong	Severe	Violent	Extreme
POTENTIAL DAMAGE	none	none	none	Very light	Light	Moderate	Moderate/Heavy	Heavy	Very Heavy
PEAK ACC.(%g)	*<.17*	*.17-1.4*	*1.4-3.9*	*3.9-9.2*	*9.2-18*	18-34	34-65	65-124	>124
PEAK VEL.(cm/s)	<0.1	0.1-1.1	1.1-3.4	3.4-8.1	8.1-16	*16-31*	*31-60*	*60-116*	*>116*
INSTRUMENTAL INTENSITY	I	II-III	IV	V	VI	VII	VIII	IX	X+

Figure 2. Predicted shaking intensity from the 1897 Assam earthquake (2a, left) and the 1905 Kangra earthquake (2b, right) determined using methodology and rupture models discussed in text. These maps are drawn from predicted pga values, which are converted to intensity according to the values given in the scale bar.

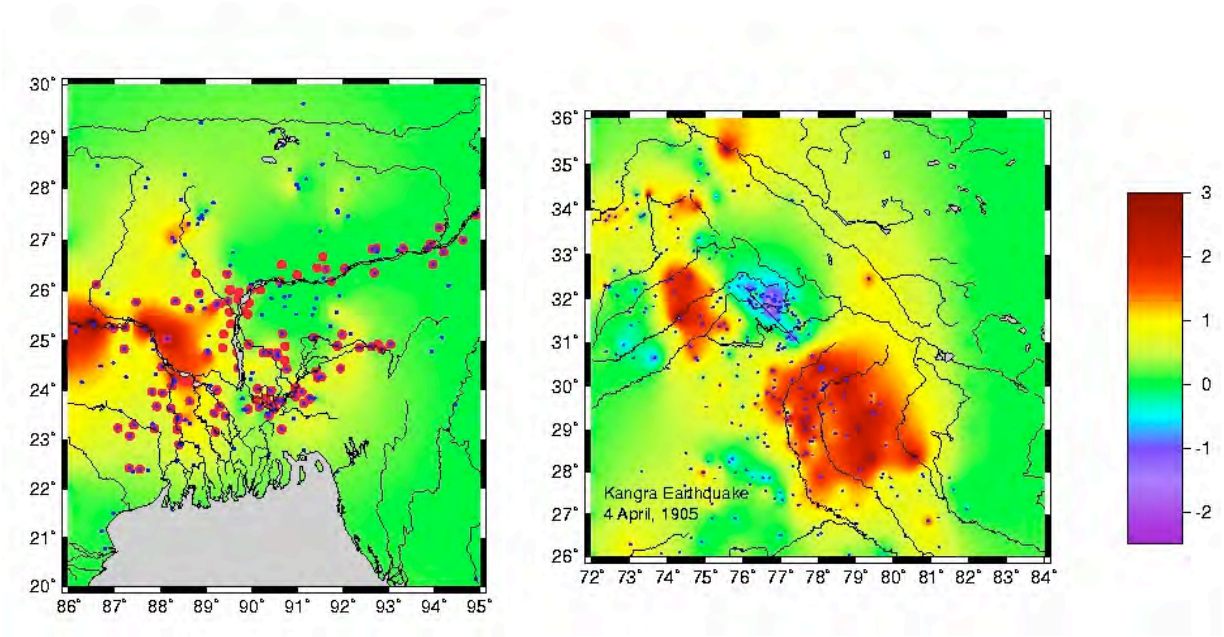

Figure 3. Residual intensity (observed minus predicted) from the 1897 Assam earthquake (3a, left) and the 1905 Kangra earthquake (3b, right) determined using methodology and rupture models discussed in text. Red circles in Figure 3b indicate sites at which liquefaction was documented. Small circles in both panels indicate locations at which intensity values were determined. The same scale bar (far left) is used to generate both figures.

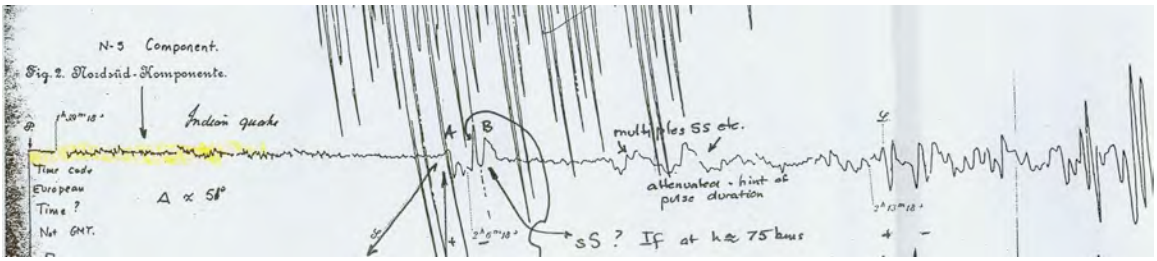

Figure 4. Recording of the 1905 Kangra mainshock made by an early Wiechert seismometer in Leipzig, Germany. The record reveals a clear initial S/sS arrival, followed by S-wave multiples with longer periods. About 7 minutes after the first S/sS arrivals, a second apparent S/sS group arrives ahead of the surface waves. The high frequency character of the second S-wave group is consistent with primary body wave arrivals from a second event but not with S-wave multiples from the first event. The second S/sS group reveals a greater S-sS time than the initial S-wave group, suggesting the second event was deeper than the first. (Note: we hope to obtain a cleaner version of this record!)

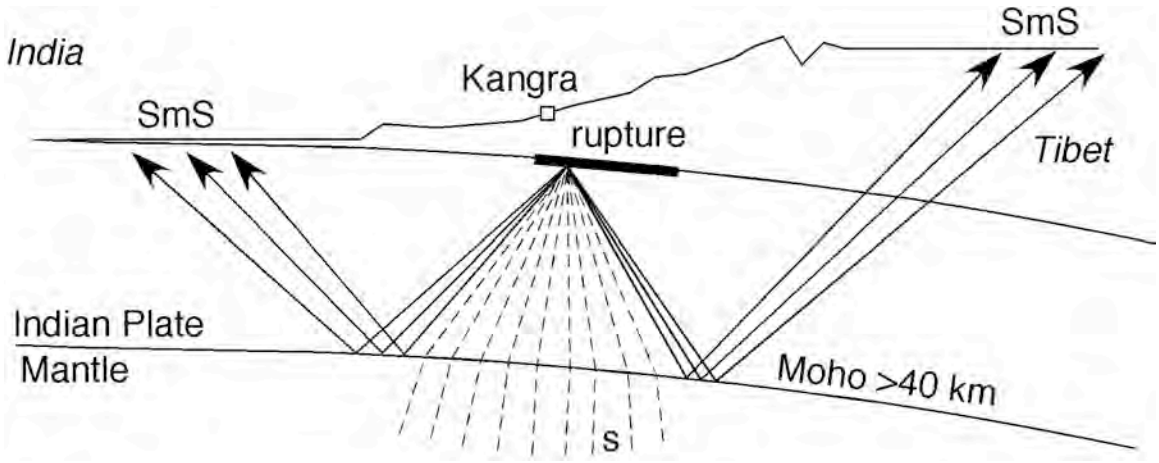

Figure 5. Cartoon illustrating the generation of post-critical SmS arrivals. If, as expected, the Moho thickens to the east of the mainshock, SmS arrivals are expected to be generated at greater distances in the Himalaya than in the direction of India.

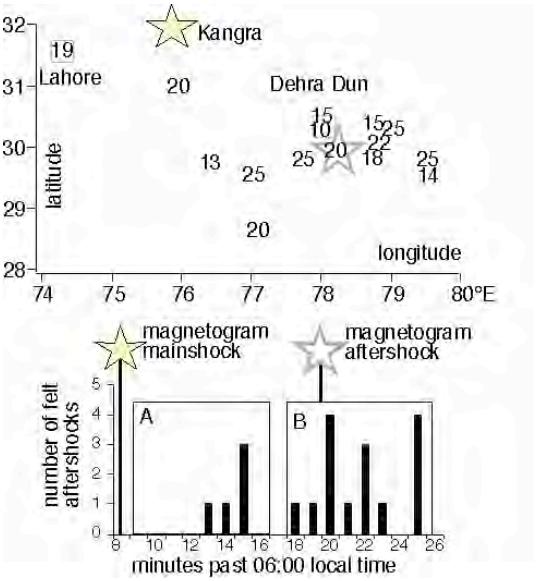

Figure 6. Map showing location and felt time in minutes of Kangra "aftershocks". Histogram below shows the clustering of these in time relative to the mainshock and aftershock recorded by a continuously recording magnetometer at Dehra Dun. The magnetogram saturated in the first 8 minutes, but a distinct arrival occurred 11.3 minutes after the mainshock. The mean and median locations for aftershocks reported in intervals A & B are all located within the star shown in map view (77.3±0.5°E, 30±0.1°N). The 14 reports that may refer to the 11.3 minute aftershock point to an epicenter at 78°E, 30°N, approximately 40 km SE of Dehra Dun.